NAVAL POSTGRADUATE SCHOOL

MONTEREY, CALIFORNIA

THESIS

SPATIAL DISTRIBUTION AND DIRECTIONALITY OF ACOUSTIC SCATTERING IN ROCKY ENVIRONMENTS

by

Amanda R. Fromm

December 2020

Thesis Advisor: Derek Olson
Second Reader: James H. MacMahan

THIS PAGE INTENTIONALLY LEFT BLANK

REPORT DOCUMENTATION PAGE	*Form Approved OMB No. 0704-0188*

1. AGENCY USE ONLY *(Leave blank)*	**2. REPORT DATE** December 2020	**3. REPORT TYPE AND DATES COVERED** Master's thesis

4. TITLE AND SUBTITLE SPATIAL DISTRIBUTION AND DIRECTIONALITY OF ACOUSTIC SCATTERING IN ROCKY ENVIRONMENTS	**5. FUNDING NUMBERS** RQNP5
6. AUTHOR(S) Amanda R. Fromm	
7. PERFORMING ORGANIZATION NAME(S) AND ADDRESS(ES) Naval Postgraduate School Monterey, CA 93943-5000	**8. PERFORMING ORGANIZATION REPORT NUMBER**
9. SPONSORING / MONITORING AGENCY NAME(S) AND ADDRESS(ES) Office of Naval Research, Ocean Acoustics program, Arlington, VA 22217	**10. SPONSORING / MONITORING AGENCY REPORT NUMBER**

11. SUPPLEMENTARY NOTES The views expressed in this thesis are those of the author and do not reflect the official policy or position of the Department of Defense or the U.S. Government.

12a. DISTRIBUTION / AVAILABILITY STATEMENT Approved for public release. Distribution is unlimited.	**12b. DISTRIBUTION CODE** A

13. ABSTRACT (maximum 200 words)

The interaction of sound, or an acoustic signal, with the seafloor is an active area of research due to its importance for naval applications in undersea warfare, mine warfare, and special operations, and for remote sensing of seafloor properties for geological and biological research. Seafloor roughness greatly affects acoustic scattering. However, little is known about how much extremely rough seafloors, such as rocky environments, affect the acoustic scattering. Rocky seafloor environments are thought to have extreme spatial variability and increased acoustic scattering compared to sand and mud seafloors. This research analyzed the spatial distribution and directionality of acoustic scattering in rocky environments to determine stationarity and isotropy. Remote sensing software often uses limited historical acoustic data to best fit the scattering parameters in a given environment. The two most common empirical models in remote sensing applications are the Lambert model and the Lommel-Seeliger (L-S) model. The L-S model proved to be a better fit to this data. The single parameter of the L-S model was used as the proxy to determine whether the scattering strength was stationary or isotropic. The measurements indicated that there was spatial variability and thus non-stationarity to the scattering behavior in both the alongshore and cross-shore directions. Scattering strength was found to be isotropic based on analysis of the survey data as a function of heading.

14. SUBJECT TERMS high frequency, sonar, acoustic, scattering, rock, rocky environment, spatial distribution, directionality, Lambert, Lommel-Seeliger, stationary, isotropic	**15. NUMBER OF PAGES** 39
	16. PRICE CODE

17. SECURITY CLASSIFICATION OF REPORT	**18. SECURITY CLASSIFICATION OF THIS PAGE**	**19. SECURITY CLASSIFICATION OF ABSTRACT**	**20. LIMITATION OF ABSTRACT**
Unclassified	Unclassified	Unclassified	UU

NSN 7540-01-280-5500 Standard Form 298 (Rev. 2-89) Prescribed by ANSI Std. 239-18

THIS PAGE INTENTIONALLY LEFT BLANK

Approved for public release. Distribution is unlimited.

SPATIAL DISTRIBUTION AND DIRECTIONALITY OF ACOUSTIC SCATTERING IN ROCKY ENVIRONMENTS

Amanda R. Fromm
Lieutenant Commander, United States Navy
BS, Eastern Illinois University, 2009

Submitted in partial fulfillment of the
requirements for the degree of

MASTER OF SCIENCE IN METEOROLOGY AND PHYSICAL OCEANOGRAPHY

from the

NAVAL POSTGRADUATE SCHOOL
December 2020

Approved by: Derek Olson
Advisor

James H. MacMahan
Second Reader

Peter C. Chu
Chair, Department of Oceanography

THIS PAGE INTENTIONALLY LEFT BLANK

ABSTRACT

The interaction of sound, or an acoustic signal, with the seafloor is an active area of research due to its importance for naval applications in undersea warfare, mine warfare, and special operations, and for remote sensing of seafloor properties for geological and biological research. Seafloor roughness greatly affects acoustic scattering. However, little is known about how much extremely rough seafloors, such as rocky environments, affect the acoustic scattering. Rocky seafloor environments are thought to have extreme spatial variability and increased acoustic scattering compared to sand and mud seafloors. This research analyzed the spatial distribution and directionality of acoustic scattering in rocky environments to determine stationarity and isotropy. Remote sensing software often uses limited historical acoustic data to best fit the scattering parameters in a given environment. The two most common empirical models in remote sensing applications are the Lambert model and the Lommel-Seeliger (L-S) model. The L-S model proved to be a better fit to this data. The single parameter of the L-S model was used as the proxy to determine whether the scattering strength was stationary or isotropic. The measurements indicated that there was spatial variability and thus non-stationarity to the scattering behavior in both the alongshore and cross-shore directions. Scattering strength was found to be isotropic based on analysis of the survey data as a function of heading.

THIS PAGE INTENTIONALLY LEFT BLANK

TABLE OF CONTENTS

THIS PAGE INTENTIONALLY LEFT BLANK

LIST OF FIGURES

THIS PAGE INTENTIONALLY LEFT BLANK

ACKNOWLEDGMENTS

I would like to thank Derek Olson, Jamie MacMahan, Mike Cook, and the entire Naval Postgraduate School Meteorology and Oceanography faculty, staff, and students, especially my cohort.

THIS PAGE INTENTIONALLY LEFT BLANK

I. INTRODUCTION

High frequency sonar (>10 kHz) can be used to remotely sense the seafloor, including bathymetry, and geoacoustic properties. This is possible because the sound field is scattered differently by the characteristics of the seafloor. This unique response by the seafloor properties is critical for naval applications that utilize acoustics such as antisubmarine warfare, mine warfare, and acoustic remote sensing in general.

An acoustic signal is a sound wave travelling through a medium, in this case, the ocean environment. The signal and its propagation through the ocean depend upon the frequency of the wave, the sound speed of the medium, particles in the water column, sea surface roughness, and seafloor roughness and composition. The seafloor varies spatially in roughness and composition but also evolves temporally due to changes caused by storms and biologics, for example (Jackson and Richardson, 2007). Seafloor sediment types range from fine muds to coarse sands to hard rock and combinations thereof. The acoustic signal interacts differently to each sediment type based on the frequency of the signal and the physical properties of the sediment (e.g., grain size, porosity, composition, density, and roughness properties). Fine-grained sediments tend to have smaller root mean square (rms) roughness, although the local hydrodynamic and biological energy is a larger factor in determining rms roughness. At low frequencies, smooth sediments, such as mud, cause the signal to reflect specularly, similar to light reflecting off a mirror. Rougher sediments, such as large-grained sand, typically cause the signal to be distributed in non-specular directions, but with most of the energy still going in the specular direction (Jackson and Richardson, 2007). The wavelength compared to the grain size is also a factor. As the wavelength becomes small, more energy is scattered outside of the specular direction.

Jackson and Richardson (2007) state that rocky seafloors cause more scattering of the acoustic signal than mud or sand sediments, likely due to their increased surface roughness. In this reference, the Lambertian empirical model (defined in Section D) was fit to previous measurements from many types of sediments. The average backscattering strength for mud seafloors follows Lambert's law curve with a Lambert scattering parameter of -19.7 dB. Sandy seafloors are also well fit by this model with an average

Lambert parameter of -20.2 dB. Even though, there is a ±5-8 dB spread in the observed scattering strengths relative to Lambert's law, it provides a good parametrization of the observed average scattering strengths of these environments (Jackson and Richardson, 2007). The rocky seafloor observations in Jackson and Richardson (2007) are limited to only three datasets, (Urick, 1954; McKinney and Anderson, 1964; APL-UW, 1994), and reports the Lambert's law backscattering value to be -5.6 dB. In Olson et al. (2016), the reported Lambert's law backscattering strengths for glacially eroded rock outcrops are -13 dB and -18 dB, which is comparable to what was reported in Gruber and Olson (2020) at -15 to -18 dB.

Knowledge of the details of the acoustic interaction with the seafloor is important to understanding the limitations and performance capability of naval sonar systems used for target detection. Environmental data are critical in order for these sonar systems to detect submarines, mines, or more generally, to distinguish hard to detect targets against a high clutter background. The Lambert (LA) model, as well as another commonly used model, Lommel-Seeliger (L-S), are based on empirical fits to measurements and can drastically over or underestimate the acoustic scattering in different types of environments and at different frequencies. Since the LA and L-S models are empirical, they have no connection to the physical properties of the environment. However, given their good fit to measurements, they are often used to characterize scattering from sediments, and can be used to summarize angle-dependent scattering strength (Harrison, 2003; Olson et al., 2016). Sand and mud seafloors have been heavily studied in terms of physical scattering models (Jackson and Richardson, 2007). However, at this point in time, physics-based models do not adequately model scattering from rocky seafloors.

A. ACOUSTIC SCATTERING OVERVIEW

This section provides a basic overview of acoustic scattering described with context focused around the seafloor geometry observed by an active acoustic system (also called an echosounder in the fisheries community). The transducer is located near the surface and acts as both the source and receiver. An echosounder that is both the source and receiver is referred to as a monostatic configuration and is the most common setup of acoustic

scattering measurements. The transducer is responsible for converting electrical signals into mechanical oscillations and acoustic waves (as the transmitter) and vice versa (as the receiver). The transmitted sound energy travels from the source, spreads spherically through the water column as a wave then interacts with the seafloor where it is scattered in all directions. The sound field backscattered by the seafloor, returns to and is measured by the receiving transducer (Figure 1).

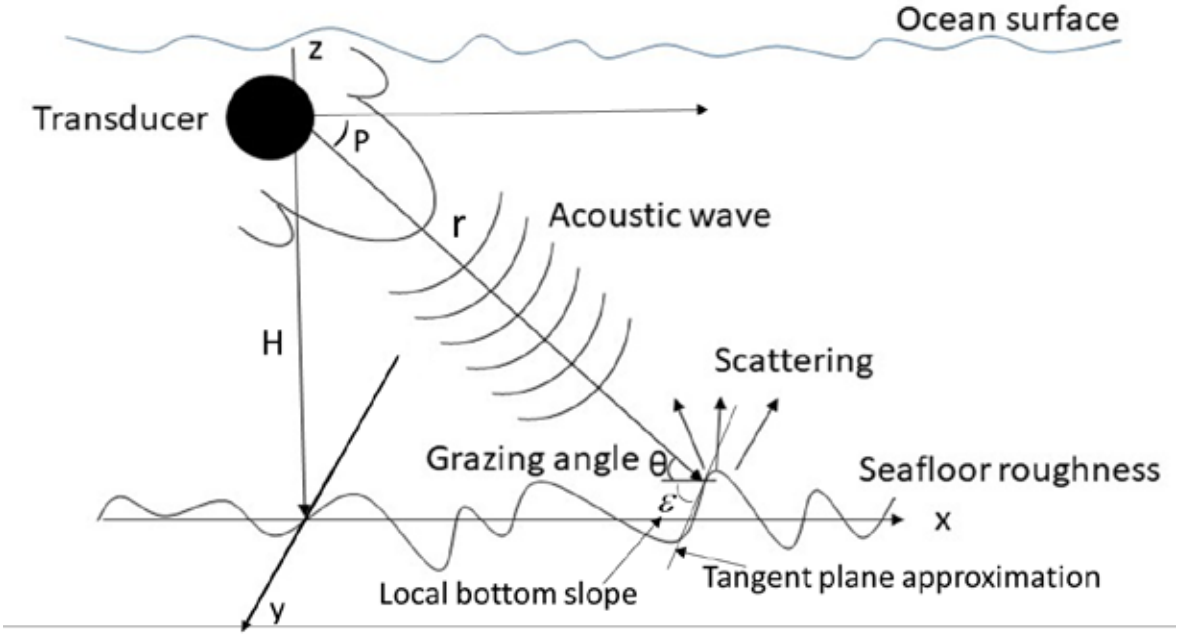

Schematic of an echosounder transmitting sound waves into the water. The sound waves interact with the rough seafloor then return to the echosounder. z is the vertical axis, y is left/right of the horizontal x axis, r is the range, H is the depth of the water, θ is the grazing angle, ε is the local bottom slope, and P is the pitch angle defined as the rotation about the y axis.

Figure 1. Acoustic overview.

The speed of the sound wave in the water column is an important aspect to ocean acoustics. Sound speed, c, is determined by the temperature, salinity, and pressure (depth) of the surrounding environment (Urick, 1983). The sound speed increases as temperature, salinity, and/or depth increases, and conversely, the sound speed decreases as those

variables decrease. In this thesis, the formulas from Fofonoff, P. and R.C. Millard Jr (1983) were used to compute sound speed from the ocean state variables.

The grazing angle, θ, is the angle between the incoming acoustic wave and the local bottom slope. For a flat seafloor, the local bottom slope, ε, is zero and the grazing angle is simply

$$\sin\theta = \frac{H}{r}, \qquad [1]$$

where H is the water depth and r is the range from the transducer to the seafloor (Figure 1). For a rough seafloor, the local bottom slope and theta are estimated differently by using the tangent plane to the rough bottom at the scale of the ensonified area of the acoustic system (Figure 1). When the signal is perfectly reflected by a flat interface, the incoming signal is reflected in the specular direction so that the incident grazing angle, θ_i, is equal to the scattered grazing angle, θ_s, although traveling in the same horizontal direction, so that the scattered wave vector is the incident wave vector, but rotated around the vertical axis (Jackson and Richardson, 2007). However, interface roughness, in the form of sediment surface variations, causes the signal to be scattered in various directions and angles. Every interaction the signal has along its path from the source to the receiver decreases its strength due to transmission loss or scattering, which include spherical spreading, attenuation, and interactions with water column inhomogeneities. The scattering interactions that occur throughout the water column include fish and elements that occur directly above or on the seafloor (e.g., rough sediment, flora, or fauna). The receiver then measures the returned intensity of the acoustic signal. This returned intensity is related to the scattering cross section of the ensonified patch of seafloor. The mathematical computations to estimate the backscattering cross section are discussed in Section C.

B. SEDIMENT PROPERTIES

The acoustic signal experiences significant distortion from interacting with the seafloor and every type of sediment affects the signal differently. The physical properties of sediments can be divided into two main categories: physical and geoacoustic (Jackson and Richardson, 2007). The physical properties of the sediment include, but are not limited

to, the sediment grain size, porosity, grain density, and mineral composition. The geoacoustic properties are related to the physical properties, but capture how the sediment affects the sound waves. These include the speed and attenuation of the waves as they propagate through the sediment, as well as the effective bulk density of the sediment / water composite medium. The spatial configuration of the sediment also affects the acoustic interaction with the seafloor. The roughness of the sediment refers to both the small scale, millimeter sized individual grains and the larger collective area of the sediment: a grain of sand versus a group of rocks.

While physics based acoustic scattering models have demonstrated accuracy at predicting acoustic behavior, they require detailed knowledge of the physical properties of the sediment, interface roughness, and fluctuations of the geoacoustic properties. Since these properties change with geographic location, which is a form of non-stationarity, it is often unrealistic to perform these small-scale physical property measurements over a wide area. Therefore, the empirical models are often used because they require less detailed information and rely on the correlation between acoustic measurements and generic descriptors of the sediment. However, empirical models can drastically over or underestimate scattering strength, especially in rocky environments. In the data discussed by Jackson and Richardson (2007), the LA model scattering strength averages -19.7 dB for mud and -20.2 dB for sand, but has a spread of $\pm$ 5-8 dB at 20^o that increases as the grazing angle increases for both mud and sand seafloors. The gravel and rock seafloors have averages of -11.7 dB for gravel and -5.6 dB for rock with a spread of $\pm$ 8-12 dB at 20^o. These variations can have significant impact on acoustic applications.

C. QUANTITATIVE METRICS OF ACOUSTIC SCATTERING

Acoustic scattering strength is related to the scattering cross section, which is a non-dimensional number that characterizes the degree of scattering from a rough interface or volume. It is independent of the measurement system (i.e., echosounder manufacturer, source level settings) and its properties, which allows for the comparison of acoustic data collected by different systems. The scattering cross section is related to the mean square scattered pressure field fluctuations scattered by the seafloor across the ensonified area.

The fluctuating pressure, P_s, has had its mean removed before forming the average. The mean square incoherent pressure is then averaged over the multiple measurements taken across the seafloor patch, and is calculated by

$$< |P_s|^2 >= |P_i|^2 A\sigma \frac{1}{r_s^2} \quad [2]$$

where $< |P_s|^2 >$ is the mean squared pressure field scattered by a patch of seafloor, $|P_i|^2$ is the squared incident pressure, A is the ensonified area, σ is the scattering cross section, and r is the distance from the ensonified area to the transducer (Jackson and Richardson, 2007). σ in this form is most correctly defined as the scattering cross section per unit area per unit solid angle (Pierce, 1981). To obtain the bottom scattering strength, S_b, the decibel equivalent of the scattering cross section, σ, is calculated by

$$S_b = 10 \log_{10} \sigma . \quad [3]$$

The form of Eq. [2] is the basis of the sonar equation [13] discussed in Section II.A.

D. ACOUSTIC MODELS

There are three commonly used statistical models that predict or estimate the seafloor roughness: the small-roughness perturbation approximation,[4], the Kirchhoff approximation, [5], and the small-slope approximation, [6].

$$\sigma = k_w^4 |A_{ww}|^2 W(\Delta K) \quad [4]$$

$$\sigma = \frac{|V_{ww}(q_{is})|^2}{8\pi} \left[\frac{\Delta k^2}{\Delta K \Delta k_z} \right]^2 I_K \quad [5]$$

$$\sigma = \frac{k_w^4 |A_{ww}|^2}{2\pi \Delta K^2 \Delta k_z^2} I_K \quad [6]$$

where the k is the wavenumber in water, K is the horizontal wavenumber, V_{ww} is the reflection coefficient, A_{ww} is a factor that depends upon the chosen wave theory and the reflection coefficient (fluid seafloor, elastic, or poroelastic), and I_K is the Kirchhoff integral, which depends on the rough interface properties, the acoustic frequency, and the measurement geometry (Jackson and Richardson, 2007).

Each of these models predicts the scattering cross section based on input parameters of statistical properties of seafloor roughness (such as the power spectrum of the roughness), and the sediment geoacoustic properties. Jackson and Richardson (2007) dedicate an entire chapter to explaining these models, and contains extensive references to the original works that derive these models. For the purpose of this paper, it is important to understand that when applied to extremely rough seafloors, such as rocks and gravel, they all perform poorly (Olson et al., 2016). This is due to all three models having restrictions to small rms seafloor height and slope. As discussed previously, rocky environments can have extreme roughness that exceeds the thresholds of these models. In addition, the roughness properties can be spatially varying, which violates the spatial stationarity assumption used by all the models for the bottom roughness (Jackson and Richardson, 2007). This is problematic since these models cannot accurately be used for remote sensing and performance prediction in rocky environments, which make up an estimated 75% of all coastlines globally (Bird, 2000).

There are two commonly used empirical models to predict seafloor roughness: the Lambert (LA) model and the Lommel-Seeliger (L-S) model. These models both model perfectly diffuse scattering from rough interfaces, and heterogeneous volumes respectively. The LA model, often referred to as Lambert's Law, appears frequently in acoustic scattering and reverberation research in order to characterize scattering measurements (Ellis et al., 1997; Jackson and Richardson, 2007). The L-S scattering model is used less often but can still provide a good fit to measured data. (Harrison, 2003; Gruber, 2019; Gruber and Olson, 2020). For both of these parameters, the scattering strength, σ , is given as a function of the model parameter, μ, and the $\sin$ of the grazing angle, θ. The difference between the LA parameter and the L-S parameter is that the $\sin$ in the denominator is to the first power for the L-S parameter [7] and is to the second power for the LA parameter [8]. The μ subscript matches to which power the $\sin$ is raised.

$$\sigma_{LS} = \mu_1 \sin^1(\theta) \quad [7]$$

$$\sigma_{LA} = \mu_2 \sin^2(\theta) \quad [8]$$

These empirical parameters allow for the comparison of the backscattering intensity for single pings or groups of pings from sonar data. For a given ping, the range of angles

accessed by the sonar may be different from other pings. These models allow for comparing two different groups of pings that may be interrogating different grazing angles. The μ value characterizes the overall level of the scattering strength of an area, which allows for a fair comparison of the behavior throughout the survey location. It should be emphasized that these two models are not based on physics, and their parameters are not related to the environment, except for empirical trends.

E. RESEARCH GOALS

The goal of this work is to add to the limited acoustic scattering observations for rocky environments and furthermore, to determine if the scattering is isotropic (even in all directions) and whether there are any directional or spatial trends to the scattering behavior. Rocky seafloors are often non-uniform in size, shape, and facet structure on individual rocks as well as entire rock outcrops. This can cause differences in the scattering values depending on the angle at which the sonar approaches the rock (Olson et al., 2016; Gruber, 2019). If the rocky seafloor properties are stationary, single passes over a rock outcrop would define the scattering values for the entire area. This study aims to determine whether small subsets of the data can account for the average scattering strength of the whole. Looking at the data collected by Gruber in 2019 in a cross-shore and alongshore coordinate reference frame provides the ability to determine if there is non-stationary behavior by looking at trends and variability to the scattering over the survey area. The data was also analyzed based on azimuthal headings to determine if there are preferential directions of elevated or reduced scattering.

These trends will help determine if acoustic scattering models should account for spatial directionality or if they can continue to assume non-stationarity and higher backscattering measurements in all rocky environments. Understanding the trends to the acoustic scattering will significantly benefit sonar applications in antisubmarine, mine warfare, and remote sensing in rocky environments.

II. METHOD

A. DATA PROCESSING

Seafloor scattering observations were collected near Asilomar Beach in Monterey, California in August 2019 using a BioSonics 200kHz split-beam echosounder. This system consists of a circular piston transducer having a beamwidth of 6.7 degrees, and tramsitted a pulse with lenth 10^{-4} s. These measurements were reported in Gruber (2019) and Gruberand Olson (2020). Five survey lines, approximately 30 minutes in length, were collected in a lawnmower type pattern. The echosounder's integrated motion sensor captured the heading, pitch, and roll (HPR) of the transducer. An integrated Garmin GPS (global positioning system) antenna with 3–5 m precision provided the geographic location of the system (Garmin, 2009). The latitude and longitude were converted into UTM (universal transverse mercator) northing and easting coordinates. The UTM positions were then rotated 64^o to define the local coordinate reference frame used throughout. An origin point in the middle of the survey area at 36.5997^o N,-121.9730^o E was designated in order to provide relative distances from the data to the origin point.

The sound velocity profile and the attenuation coefficient were calculated using the echosounder frequency and the local environmental data (Fofonoff and Millard, 1983; Jackson and Richardson, 2007). The environmental data were measured by the local Scripps Buoy 46240 and the NOAA National Data Buoy Center (NOAA National Data Buoy Center). Sound velocity was used to convert the time of the received pulse into the the range, r, from the transducer to the seafloor. The depth, H, was calculated using

$$H = r \sin(-P) \quad [9]$$

where r is the range and P is the pitch angle defined as the rotation about the y axis (Figure 1). This is nominally the negative of angle from the horizontal, since only angles below horizontal are used here. The location of the ensonified patch of seafloor was calculated based on the location of the transducer by calculating the horizontal distance, x, from the transducer to the seafloor using

$$x = r \cos(-P) \quad [10]$$

The grazing angle, θ, is calculated by

$$\theta_o = -P + \gamma \quad [11]$$

where γ is the vertical channel of the split beam sonar. Integrating the local bottom slope, ε, into the grazing angle estimation makes the equation

$$\theta = -P + \gamma + \varepsilon \quad [12]$$

The sonar equation was used to calculate the acoustic backscatter strength, S_b.

$$S_b = 10\log_{10}(V^2/2) - SL - RS - D_x - D_r + 2\alpha r_t + 30\log_{10}(r_t/r_{ref}) - 10\log_{10}(c_w \tau \Psi / 2 r_{ref}) \quad [13]$$

where S_b is the backscatter strength, V is the voltage output of the echosounder processor (with units of counts), SL is the source level (dB), RS is the receiver sensitivity (dB), D_x and D_y are the beam patterns in the x and y directions, α is the attenuation coefficient, r_t is the relationship between range and time, c is the speed of sound in sea water, τ is the pulse length, and Ψ is the effective angular width of the incident beam projected onto the seafloor (Jackson and Richardson, 2007). Using the definition of Ψ from Jackson and Richardson (2007) includes an effective factor of $\frac{1}{\cos(\theta)}$ that is used in other forms of the sonar equation. Each ping was then decimated in time by a factor of 4 (due to oversampling), smoothed, and averaged.

The error for the data is based primarily on upon the system calibration. The uncertainty in the source level and receiver sensitivity is the largest source of error. Other small and insignificant sources of error include the finite sample size, the angle accuracy, the location accuracy, and the beam pattern. The total error in the data was determined to be +/- 2 dB.

B. EMPIRICAL MODEL FIT

The data were analyzed as a function of grazing angle, summarized over large spatial averages to determine which empirical model fit better, LA or L-S. Backscattering strength is compared against the LA and L-S models discussed in Section I.D in Figure 2.

The horizontal axis is the grazing angle, q, in degrees and the vertical-axis is the backscattering strength in dB. The average backscatter strength for this data is -16.4 dB over all angles, and is plotted as a solid black horizontal line. Both the LA and L-S parameter curves are plotted as dotted and dashed lines, respectively. Each solid color survey line represents one survey line, approximately 30 minutes worth of data. The scattering strength as a function of grazing angle line plots on the graph were created by averaging the backscattering strength of all (thousands) of pings per grazing angle.

The scattering values at 20^o are approximately 2 dB from the L-S curve and approximately 4–6 dB from the LA curve. The misfit is less pronounced between the scattering values and each model as the grazing angle increases (Figure 2). However, based on this evidence, the L-S model provides a better representation of the scattering behavior for this data. This conclusion framed the spatial variability and directionality analysis, and the decision was made to use the L-S parameter, m_l, as a proxy for the analysis. The proxy is necessary because the grazing angle accessed by each ping is different, and it would be otherwise difficult to compare different measurements made along the survey track. This parameter is examined later in more detail using fewer data in the averaging ensemble so that smaller scales may be resolved.

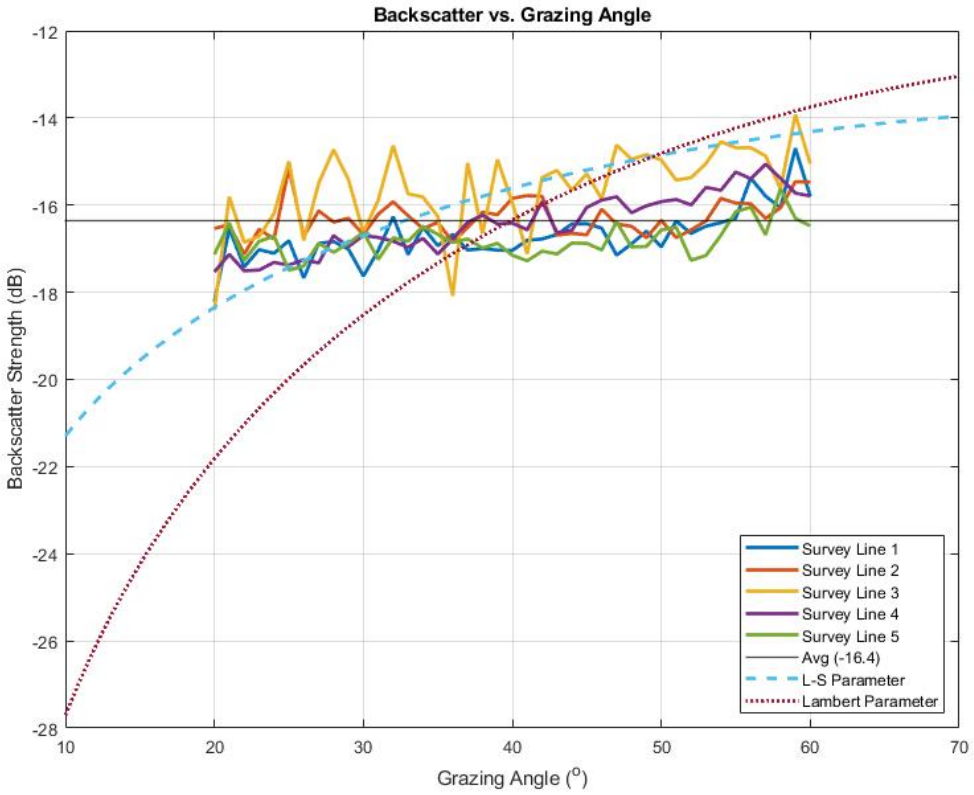

The acoustic backscatter as a function of grazing angle compared to the Lommel-Seeliger (L-S) and Lambert (LA) scattering parameters. The L-S parameter is a better fit for this data.

Figure 2. Acoustic backscatter as a function of grazing angle for each survey line plotted with the L-S and LA model comparisons.

C. SPATIAL VARIABILITY

To determine if there was a spatial trend based on the L-S, η, scattering parameter, the angle of the natural coastline was used to define local cross- and along-shore coordinates. Asilomar Beach runs at an approximately 30º angle compared to geographic north in the vicinity of the data site (Figure 3). Since the data were collected using a back and forth lawnmower type pattern, the data mostly runs parallel (alongshore) or perpendicular (cross-shore) to the coastline. For the basis of this research, alongshore is defined as heading directions of 30º and 210º and cross-shore is defined as heading directions of 120º and 300º (Figure 3).

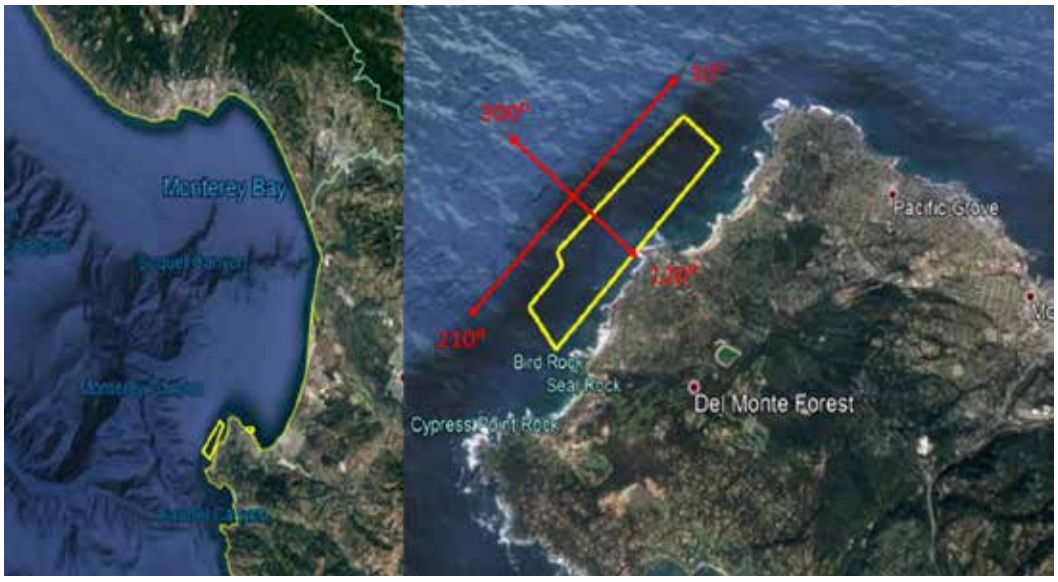

Data were collected within the yellow box in a lawnmower type pattern near Asilomar Beach Monterey, CA in 2019. The beach is angled approximately 30º from north. Alongshore headings are 30º and 120º and cross-shore headings are 120º and 300º.

Figure 3. Source data location: Asilomar Beach Monterey, CA.

The L-S η parameter was estimated from a subset of binned and averaged pings over the entire survey area. The alongshore scattering values were binned by increments of 10 m spacing and the cross-shore scattering values were binned by increments of 5 m spacing due to the amount of available data in each direction.

D. DIRECTIONALITY

The L-S η parameter was binned by increments of five degrees and averaged then analyzed to determine if a trend existed for any specific direction or directions based on azimuthal headings. The L-S parameter was calculated and compared to all headings to determine isotropy for the scattering behavior.

THIS PAGE INTENTIONALLY LEFT BLANK

III. RESULTS

Overall, this study found that there is variability to the scattering behavior across the survey area, but does not favor any particular direction. Spatially, the scattering strength seemed to be consistent in strength in both the alongshore and cross-shore directions with no trend towards either direction. However, within the alongshore and cross-shore positions there are areas of increased and decreased scattering (more so for the alongshore positions). For the directionality, or azimuthal dependence, this study revealed that the scattering is isotropic, with no trend towards any heading.

A. SPATIAL VARIABILITY

Based on the dependence of the L-S parameter as a function of the alongshore and cross-shore position, there is variability to the scattering strength across the survey area. The μ_1 values in Figure 4 are shaded from lower values in teal to higher values in pink. The color bar was cut off at a minimum value of -25 dB. Any μ_1 values less than -25 dB are bright teal. The black and white background image is the detrended bathymetry data from California State University Montery Bay Seafloor Mapping Lab: South/Central Monterey Bay-Asilomar (2009–2010). A mean plane was subtracted to remove the general across shore slope, and to more effectively display smaller scale roughness features. Lighter colors indicate shallower areas and the darker colors indicate deeper areas with the scale on the left indicating relative seafloor height. The values do not represent actual depth since a mean plane has been subtracted from these data. The plot has been rotated so that the alongshore direction is shown horizontally left to right and the cross-shore direction is shown vertically up and down. The alongshore distance and average μ_1 values are plotted horizontally at the bottom and the cross-shore distance and averaged μ_1 values are plotted vertically on the right side. The alongshore and cross-shore distances are the relative distance from the data ping location on the seafloor to the origin point discussed in Section II.A.

The alongshore pings were binned based on distance from each other. Groups of pings that were within 10 meters were binned together. The cross-shore pings were binned by 5 meter increments because there are fewer data points in the cross-shore direction. There is very little variability to the cross-shore scattering. However, the alongshore plot indicates increased variability. The brighter colors on the graph and the lower scattering values on the alongshore plot seem to align in or near survey track turns (Figure 4).

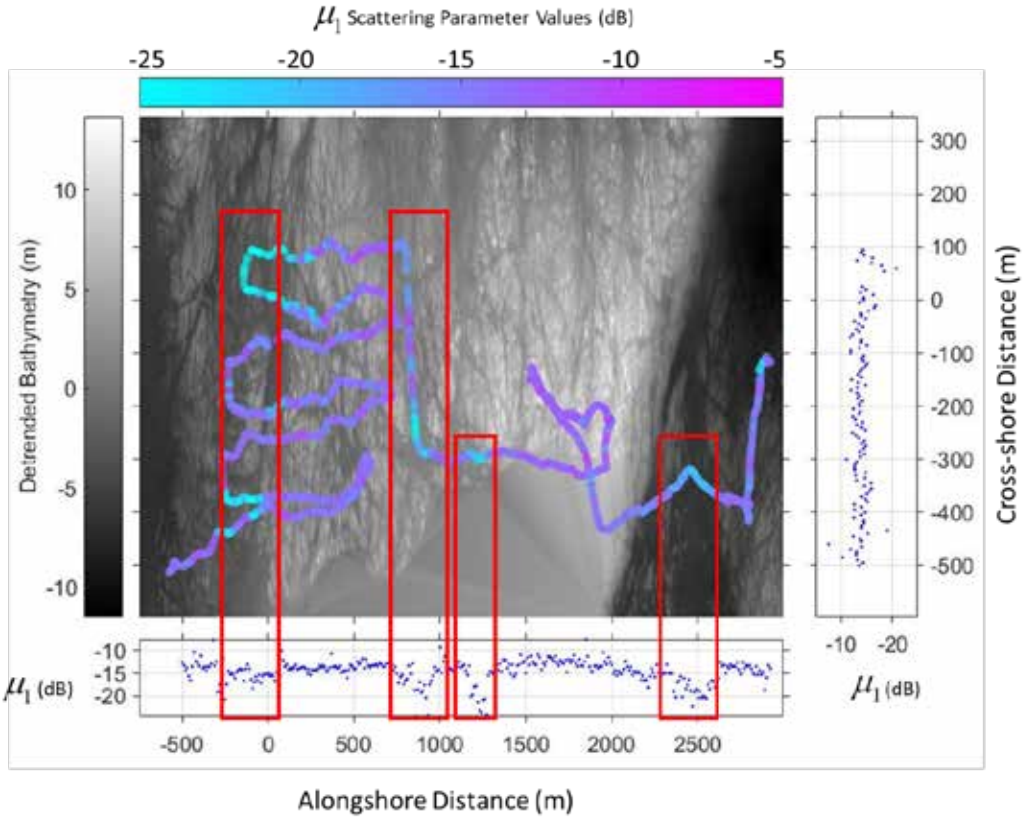

L-S scattering parameter values overlaid on black and white detrended bathymetric data. The alongshore μ_1 scattering strength values are on the bottom and the cross-shore L-S scattering values are on the right. The red boxes align areas of lower scattering values on the bathymetric image and alongshore plot.

Figure 4. Alongshore and cross-shore mu1 scattering values over the local bathymetry.

The η scattering parameter in both the alongshore and cross-shore directions described above and shown in Figure 4 is shown in a little more detail in Figure 5. The x-

axis is the alongshore or cross-shore distance from the origin point in the survey area and the y-axis is the μ_1 scattering parameter in dB. The ± 2 dB error discussed in Section I.A are shown in blue and red. The average alongshore μ_1 is -14.0 dB, and the average cross-shore μ_1 is -13.8 dB. The difference in the averages is likely due to differences in the averaging of the pings, the total amount of pings available in each direction, and the averaging of the μ_1 parameter rather than the averaging of the scattering strength. There are significantly more data points in the alongshore direction between the distances of approximately -300 m to 700 m due to the lawnmower survey pattern. There seems to be less variation in that segment of the data due to the averaging. However, there are local minima at approximately -300 m, 800 m, 1300 m, and 2500 m on the alongshore plot which are also highlighted by the boxed regions in Figure 4.

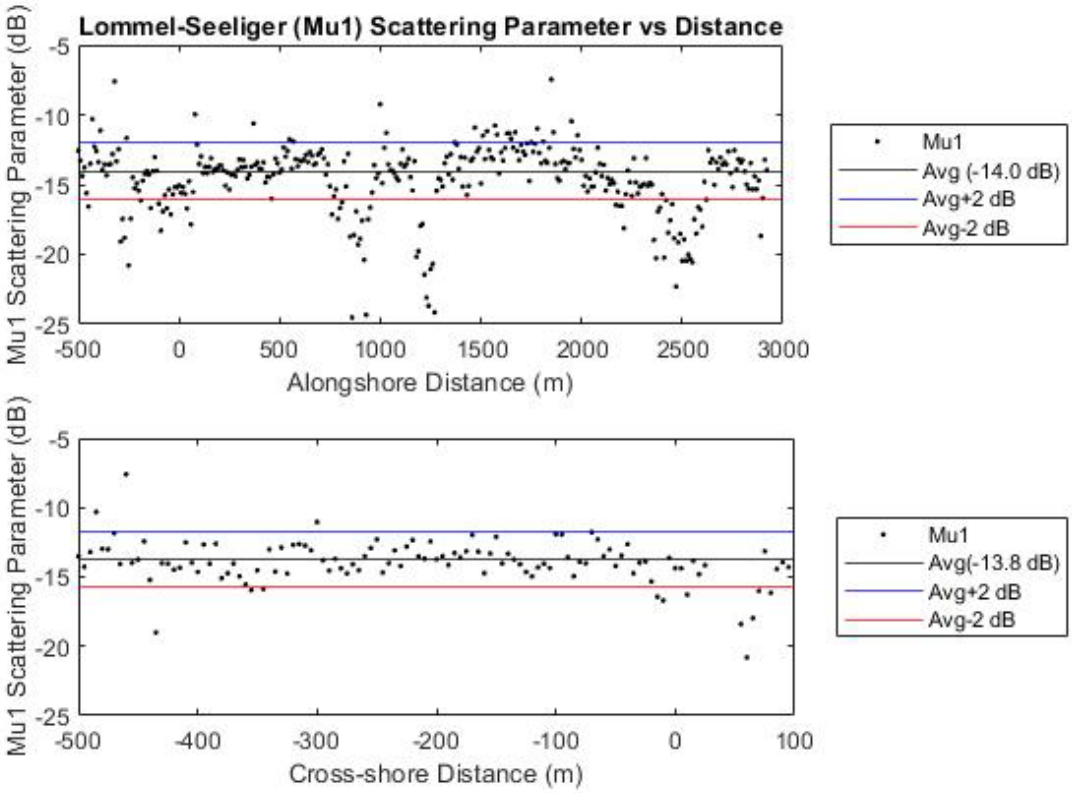

The acoustic scattering in both the alongshore and cross-shore directions are spatially variable but the average scattering value is similar.

Figure 5. Alongshore and cross-shore scattering values.

There are several possible explanations to the areas of increased and decreased scattering. It is possible that there is less scattering variability in the turn because as the sonar pivots around that point, more pings are averaged in those areas. This averaging would decrease the spread of the backscatter strengths associated with individual pings, but have little effect on the overall scattering strength. It is possible that there is a change in the acoustic geometry due to changes in the orientation of the boat in the turns. If the boat leans into the turns, the grazing angles accessed by the pings could be on average lower or higher depending on which way the boat leans. We know that the backscatter strength changes as a function of grazing angle and that the backscatter strength changes more rapidly for lower grazing angles than it does for the higher angles (Figure 2). The empirical models are also less accurate at lower angles. Another possibility for decreased scattering values is that there are areas of a more sand or mud composite seafloor. However, the resolution of the bathymetric image is too coarse to determine if there are significant features (or lack thereof) that align with the areas of higher or lower scattering values (Figure 4). Biological activity is another possible explanation to the variability throughout the survey area. Any source of roughness (e.g., rock shape or biologics), can be a source of increased scattering depending on their size compared to the relative wavelength. In this case, the wavelength is on the sub 10 mm scale and since these small scale wavelengths are not resolved in the grid, it is impossible to make these inferences. Unfortunately, this analysis does not provide data to answer why there are areas of increased and decreased scattering throughout the survey area; it only shows that the variability to the scattering behavior exists across the survey area. The spatial variability, however, does not appear to have widespread systematic trends throughout the survey area.

B. DIRECTIONALITY

The L-S parameter, μ_1, for this dataset was found to be mostly constant as a function of azimuth, and thus isotropic. No indication of a directional scattering trend associated with any particular heading was found (Figure 6, Figure 7). The m_l scattering parameter for all heading directions is shown in Figure 6 where the x-axis is the heading direction in degrees and the y-axis is the scattering strength in dB. The average scattering strength for

all headings is -13.7 dB and is shown by the solid black line. The ± 2 dB error are shown by the blue and red lines. Both Figure 6 and Figure 7 show that there is variation to the scattering strength, but there is no trend to the scattering in favor of any direction or heading.

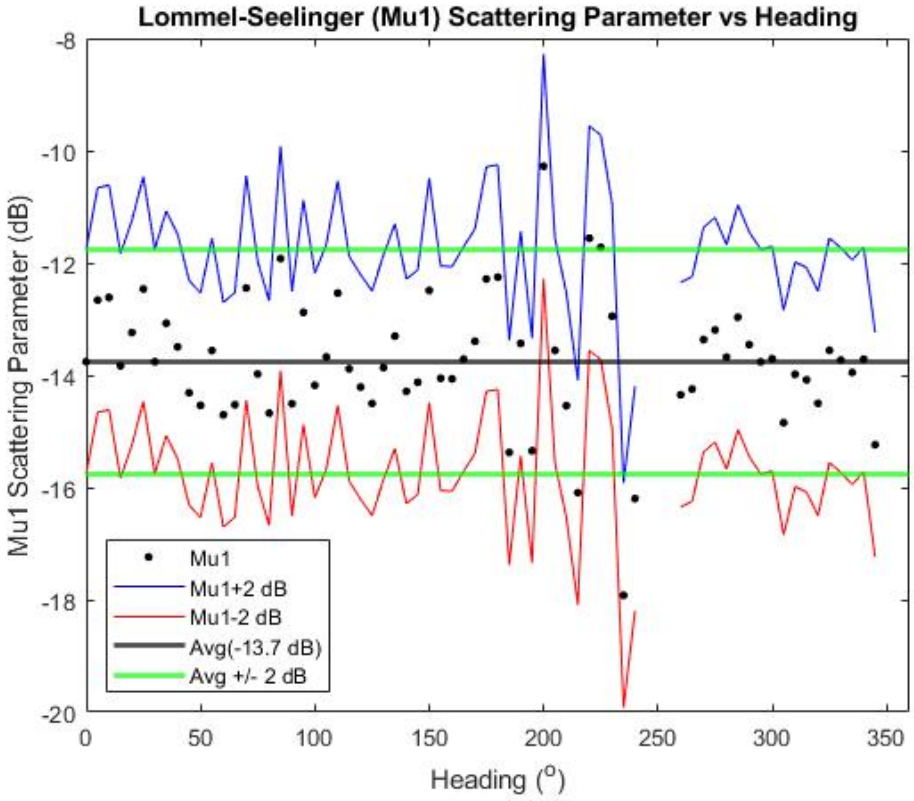

The L-S scattering parameter has no directional trend toward any heading. The average error of +/- 2dB and the average scattering strength is included to understand the error associated with the variability.

Figure 6. L-S scattering strength compared to heading.

The polar plot in Figure 7 shows a scaled L-S parameter compared to all headings. An arbitrary value of 20, $10\log_{10}(m_1)+20$, was added to the scattering strength values shown in Figure 5 and Figure 6 in order to make the values positive for the polar plot. Similar to Figure 6, the m_1 values are plotted against the heading direction and the ± 2 dB standard deviations are plotted in red and blue. The alongshore and cross-shore directions

are highlighted by the grey shading. The alongshore and cross-shore directions were highlighted as a clear visual reminder of the local coordinate reference frame and to more easily determine if those directions were a basis for a scattering trend. The polar plot demonstrates very clearly that there is no directional trend to the scattering in this area within the uncertainty of the measurements.

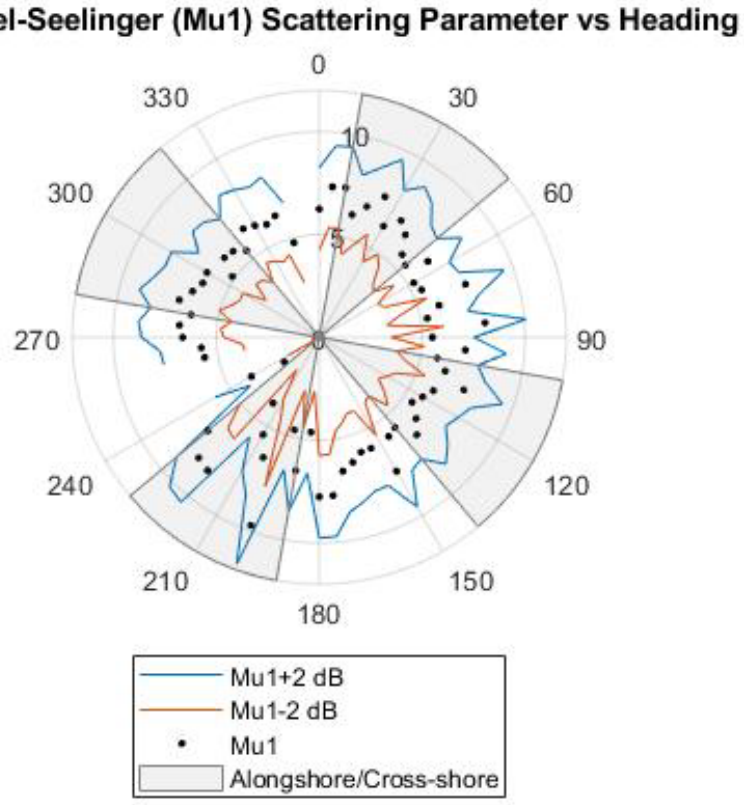

The polar plot of the η_1 scattering parameter compared to headings provide a better understanding that there is no directionality to the data. The alongshore and cross-shore directions are highlighted within the gray area on the plot. An arbitrary value of 20 was added to the η_1 values to make them positive on this plot.

Figure 7. L-S scattering strength polar plot for all headings.

IV. CONCLUSION

Based on the comparison of the backscatter strength with the grazing angle for this data, the Lommel-Seeliger (L-S) scattering parameter, μ, was chosen as a proxy for scattering strength to study spatial variability and directionality. The L-S parameter, μ, was binned and averaged based on the distance between the pings and the selected origin point in both the alongshore (parallel to the coast) and cross-shore (perpendicular to the coast) directions to determine the spatial variability throughout the survey area.

It was determined that there is spatial variability to the scattering in both alongshore and cross-shore directions, and that there is a larger spread to the scattering values alongshore than cross-shore (Figure 5). The μ averages for the alongshore and cross-shore positions were similar and likely only differ due to averaging. The variation compared to the alongshore average was $\pm$7-10 dB with the majority of the data points falling within the $\pm$2 dB uncertainty error. There is less variation to the cross-shore data at $\pm$6-8 dB and again with most of the data points falling within the $\pm$2 dB uncertainty error. (Figure 5). The lack of consistency in the acoustic scattering strength throughout the survey area makes the scattering behavior non-stationary in space.

The μ was then discretized against compass headings. The scattering values indicate that there is no directional trend to this data. Similarly, to the spatial variability, there is directional variability to the L-S scattering parameter. However, no systematic trend, to within the uncertainty of the measurements, was found. The majority of the scattering values fall within the $\pm$2 dB uncertainty when compared against heading directions (Figure 6 and Figure 7). Since there is no trend towards any direction, the scattering behavior is isotropic in this rocky environment.

The spatial variability of the scattering strength of this area was expected since it is a rocky coastal environment with large roughness. This analysis determined that the scattering does not favor any particular direction or position within the survey area. This indicates that the scattering in rocky environments is non-stationary and isotropic. These

results align with the higher scattering values found in recent acoustic research of rocky environments. Adding these scattering values alongside other comparisons to empirical models will aid in remote sensing applications to find or detect submarines, underwater mines, or assist in target acquisition of underwater weapons systems.

LIST OF REFERENCES

APL-UW, 1994: *High-Frequency Ocean Environmental Acoustics Models Handbook.* Seattle: Applied Physics Laboratory University of Washington.

Bird, E., 2000: *Coastal Geomorphology: An Introduction.* John Wiley & Sons.

California State University Montery Bay seafloor mapping lab: South/Central Monterey Bay-Asilomar, 2009–2010. Retrieved June 01, 2018, from http://seafloor.otterlabs.org/SFMLwebDATA_mb.htm#MONT

Ellis, D., J. R. Preson, R. Hollet, J. Sellschopp, 1997: Analysis of towed array reverberation data from 160 to 4000 Hz during Rapid Response 97. SACLANT Undersea Research Centre. Retrieved from https://apps.dtic.mil/dtic/tr/fulltext/u2/a389980.pdf

Fofonoff, P. and R.C. Millard Jr., 1983: Algorithms for computation of fundamental properties of seawater. *Unesco Tech. Pap. in Mar. Sci.*, **44**, 53.

Garmin, 2009: GPS technical specifications. Retrieved October 8, 2020, from https://static.garmin.com/pumac/GPS15xH_15xL_TechnicalSpecifications.pdf

Gruber, J., 2019: Measurements of acoustic scattering from rocky outcrops in Monterey Bay. M.S. thesis, Department of Oceanography, Naval Postgraduate School.

Gruber, J., and D. Olson, 2020: Measurements of acoustic scattering from rocky seafloors using a split-beam echosounder. Unpublished Manuscript, Naval Postgraduate School, Department of Oceanography.

Harrison, C., 2003: Closed-form expressions for ocean reverberation and signal excess with mode stripping and Lambert's law. *J. Acoust. Soc. Amer.*, **114**. Retrieved from https://asa.scitation.org/doi/abs/10.1121/1.1618240

Jackson, D. R., and M. D. Richardson, 2007: *High-Frequency Seafloor Acoustics.* New York: Springer.

McKinney, C. M., and C. D. Anderson, 1964: Measurement of backscattering of sound from the ocean bottom. *J. Acoust. Soc. Amer.,* **36**, 158–163. doi:10.1121/1.1918927

NOAA, 2019: National Data Buoy Center. Retrieved August 02, 2019, from https://www.ndbc.noaa.gov/

Olson, D. R., A. P. Lyons, and T. O. Sæbø, 2016: Measurements of high-frequency acoustic scattering from glacially eroded rock. *J. Acoust. Soc. Amer.,* **139**, 1833–1847. doi:10.1121/1.4945589

Pierce, A., 1981: *Acoustics: An Introduction to its Principles and Applications.* New York: McGraw-Hill Book Co.

Urick, R. J., 1954: Measurement of sound from a harbor bottom. *J. Acoust. Soc. Amer.*, **26**, 231. doi:10.1121/1.1907314

Urick, R. J., 1983: *Principles of Underwater Sound* (3rd ed.). Los Altos Hills: Peninsula Publishing.

INITIAL DISTRIBUTION LIST

1. Defense Technical Information Center
   Ft. Belvoir, Virginia

2. Dudley Knox Library
   Naval Postgraduate School
   Monterey, California